AIP Journal of Applied Physics

Defect and nanocrystal cathodoluminescence of synthetic opals infilled with Si and Pt

C. Díaz-Guerra, D. A. Kurdyukov, J. Piqueras, V. I. Sokolov, and M. V. Zamoryanskaya

Citation: J. Appl. Phys. **89**, 2720 (2001); doi: 10.1063/1.1346653
View online: http://dx.doi.org/10.1063/1.1346653
View Table of Contents: http://jap.aip.org/resource/1/JAPIAU/v89/i5
Published by the AIP Publishing LLC.

Additional information on J. Appl. Phys.

Journal Homepage: http://jap.aip.org/
Journal Information: http://jap.aip.org/about/about_the_journal
Top downloads: http://jap.aip.org/features/most_downloaded
Information for Authors: http://jap.aip.org/authors

Downloaded 11 Oct 2013 to 147.96.14.16. This article is copyrighted as indicated in the abstract. Reuse of AIP content is subject to the terms at: http://jap.aip.org/about/rights_and_permissions

Defect and nanocrystal cathodoluminescence of synthetic opals infilled with Si and Pt

C. Díaz-Guerra
Departamento de Física de Materiales, Facultad de Físicas, Universidad Complutense, E-28040 Madrid, Spain

D. A. Kurdyukov
Ioffe Physico-Technical Institute, RAS, 194021 St. Petersburg, Russia

J. Piqueras[a]
Departamento de Física de Materiales, Facultad de Físicas, Universidad Complutense, E-28040 Madrid, Spain

V. I. Sokolov and M. V. Zamoryanskaya
Ioffe Physico-Technical Institute, RAS, 194021 St. Petersburg, Russia

(Received 29 September 2000; accepted for publication 7 December 2000)

Synthetic opals—composed of 250 nm amorphous silica spheres closed packed in a face centered cubic structure—have been infilled with silicon, platinum, and with Si and different Pt contents. The luminescent properties of these composites have been investigated by cathodoluminescence (CL) microscopy and spectroscopy. CL emission is influenced by the material used to infill the pores of the opal matrix. CL spectra of all the samples investigated show two well-known bands, associated with the defect structure of the silica spheres, centered at about 1.9 and 2.7 eV, respectively. Emission in the 2.15–2.45 eV range, particularly intense in opal-based composites with a high Pt content, is tentatively associated with SiO_2 defects involving silicon clusters. A CL band peaked at about 3.4 eV as well as a band in the 1.50–1.75 eV range, whose peak position seems to be affected by the Pt content of the samples, are associated with the presence of Si nanocrystals. The behavior of these emissions suggests that both are related to defect states at the interface between Si nanocrystals and SiO_2 forming the opal spheres. © *2001 American Institute of Physics.*
[DOI: 10.1063/1.1346653]

I. INTRODUCTION

Three-dimensional assemblies of semiconductor nanodevices with a high volume density of active elements will be required by solid-state electronics technology in the near future. Synthetic opals possess a regular sublattice of channels and voids that can be infilled with different materials in order to create such nanostructures using the so-called matrix technology. The use of opals infilled with semiconducting materials is also a subject of interest in optoelectronics due to the application of these composites as photonic crystals.[1–3]

Opals are made of closed-packed amorphous submicron silica spheres forming a fcc lattice. It is known that the defect structure of SiO_2 is sensitive to ionizing radiation.[4,5] Irradiation produces defects by either electron or hole trapping at preexisting precursors defects, which are strongly dependent on the sample stoichiometry. Alternatively, atomic displacements from defect-free sites can result from radiolytic processes. Many SiO_2-based devices could be operated in radiation environments, therefore the characterization of the radiation sensitive defect structure of opals is of great importance to enable optimum device design.

Cathodoluminescence (CL) in the scanning electron microscope (SEM) is a well-established technique for the defect characterization of semiconducting and semi-insulating materials. While photoluminescence (PL) has been widely applied to the study of the emission properties of SiO_2 or Si-based nanostructures, e.g., Refs. 6–8, CL has not been so frequently applied to the characterization of these materials.[5,9,10] The aim of this article is to use the CL for optical and structural characterization of synthetic opals infilled with silicon (opal:Si), platinum (opal:Pt), and opals infilled with Si and different Pt contents (opal–Pt–Si). CL of bare opals will also be studied and compared with those of infilled samples. In particular, we investigate not only the defect CL emission of the opals but also the CL emission related to Si nanocrystals, which are formed in some of the samples. Both luminescence of Si-based heterostructures and luminescence of silicon nanocrystals are subjects of increasing interest due to potential integration of this material in optoelectronic devices. Influence of electron beam excitation conditions and thermal annealing on the luminescence of the opal-based composites will be addressed as well. In addition, the effects of Si and Pt distribution inside the opal pores on the CL emission have been also investigated. The obtained results will be correlated with previous transmission electron microscopy (TEM) observations and Raman measurements.

II. EXPERIMENT

The opal samples investigated in this work consist of fcc-packed amorphous silica spheres of about 250 nm diameter. The sizes of the octahedral and tetrahedral voids that

[a]Electronic mail: piqueras@eucmax.sim.ucm.es

 © 2001 American Institute of Physics

Downloaded 11 Oct 2013 to 147.96.14.16. This article is copyrighted as indicated in the abstract. Reuse of AIP content is subject to the terms at: http://jap.aip.org/about/rights_and_permissions

exist in this lattice are approximately 100 and 50 nm, respectively. A 26% of the total matrix volume is accessible for filling with other substances. The density of the bare opals samples is 1.1 g/cm^{-3}. The opals are prepared by sedimentation of synthetically grown monodispersed spherical SiO_2 globules obtained by hydrolysis of tetraethoxysilane in the presence of ammonium hydroxide.[11] The silica spheres are not continuous solids but consist of several closed-packed spheres of smaller diameter (~40 nm), which in turn are made of particles of about 10 nm in size.[12] Hence, there is a substructure inside the SiO_2 spheres. After sedimentation, the opals are hardened by hydrothermal annealing. During this process most of the smaller globules result partially coagulated and a porous disordered structure appears inside the silica spheres, as revealed by TEM observations.[13]

Silicon was incorporated into opal (opal:Si samples) by a thermal chemical vapor deposition technique following the procedure described in Ref. 14. It has been previously observed[15,16] that annealing modifies the structure of the as-grown Si layer in the opal:Si samples. In order to investigate the effects of this treatment in the luminescent properties of the opals and opal:Si composites some of these samples were annealed at 800 °C in air under about 1 Torr pressure. Embedding of Pt in the opal matrix (opal:Pt samples) was carried out by a multicyclical method in which opals were impregnated with a saturated solution of platinum tetrachloride in ethanol and then $PtCl_4$ was reduced with hydrogen. Opal–Pt–Si composites were prepared embedding the opals first with platinum and then with silicon. These treatments lead to opal structures with the pores partially filled, due to coating of the spheres, with Si, Pt, or both elements, respectively. In the latter case the fraction of Si and Pt was estimated as described later.

The morphology of the opal-based composites was investigated in a Leica Stereoscan 440 SEM. CL observations were carried out in the 300–1200 nm spectral range using either a Camebax electron microprobe analyzer or a Hitachi S-2500 SEM. Details of the experimental setup used for CL images and spectra acquisition have been reported elsewhere.[17,18] Measurements were performed at accelerating voltages ranging from 10 to 25 kV, beam currents ranging from 1 to 50 nA and temperatures between 85 and 295 K.

The Si and Pt fill factors of the opal pores have been evaluated by x-ray microanalysis at different depths in cross sections of the samples. The Si concentration measured includes not only the material embedded into the opal pores but also Si from the amorphous SiO_2 forming the opal spheres. This latter concentration of Si equals, in atomic %, to half of the oxygen concentration (K_O). Therefore, the concentration of silicon embedded in the opal pores (K_{Si}) can be expressed, in atomic %, as

$$K_{Si} = K_{Si}^{*} - 1/2 K_O,$$

where K_{Si}^{*} is the total Si concentration in atomic %. The same concentration expressed in weight % (C_{Si}) is given by

$$C_{Si} = K_{Si} C_{Si}^{*},$$

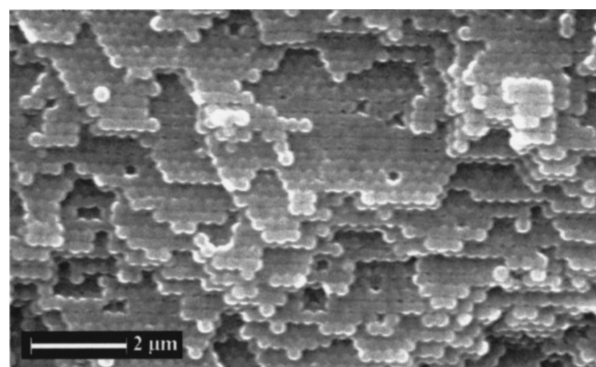

FIG. 1. SEM image of an opal sample.

where C_{Si}^{*} is the total Si concentration in weight %. The Si and Pt fill factors of the opal pores, in volume %, were then evaluated using the following expression:

$$X = 100\% \, (C_k/\rho_k)/(C_{opal}/\rho_{opal})/0.26.$$

C_k and C_{opal}, respectively, represent the concentrations of the element considered (Pt or embedded Si) and the SiO_2 that forms the opal, while ρ_k and ρ_{opal} are the corresponding densities.

III. RESULTS

A. Bare opals

SEM images of the opals show compact and well-ordered layers of SiO_2 spheres of about 250 nm of diameter (Fig. 1). As in all the samples investigated in the present work, CL intensity (I_{CL}) in the visible spectral range increases by increasing irradiation time until a saturation is reached. In this condition three emission bands centered at about 1.95, 2.7, and 3.35 eV are clearly resolved (Fig. 2). Gaussian deconvolution of the obtained spectrum reveals the existence of four bands centered at 1.97, 2.35, 2.66, and 3.37 eV. No significant change in the $I_{CL}(1.9\,eV)/I_{CL}(3.4\,eV)$ ratio was found by increasing irradiation time, while an enhancement of the CL intensity in the (2.4–2.8) eV range was clearly observed. Upon annealing at 800 °C a higher luminescence intensity was appreciated. Spectra show two well

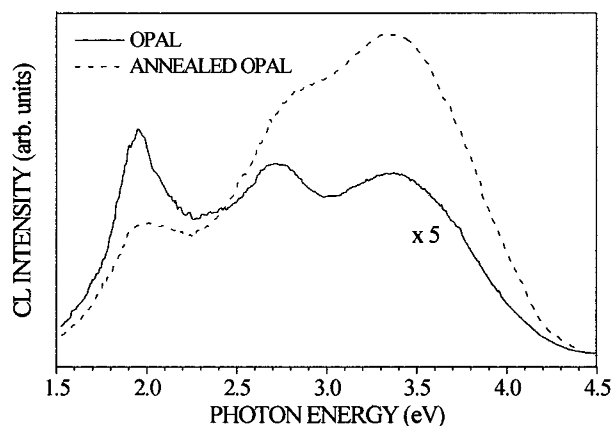

FIG. 2. CL spectra of bare opal and annealed opal samples (15 kV, 1 nA, 295 K).

Downloaded 11 Oct 2013 to 147.96.14.16. This article is copyrighted as indicated in the abstract. Reuse of AIP content is subject to the terms at: http://jap.aip.org/about/rights_and_permissions

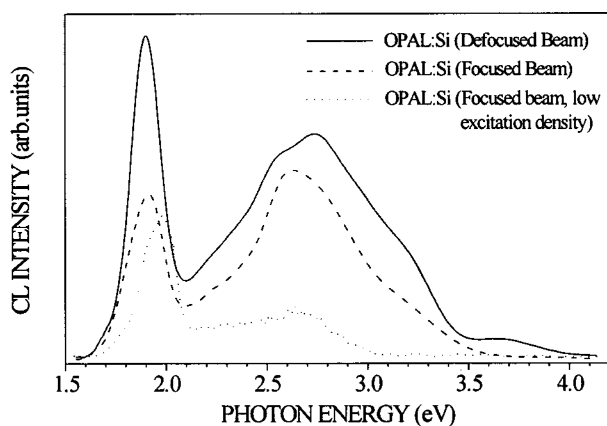

FIG. 3. CL spectra of annealed opal:Si recorded under three sets of excitation conditions: Low excitation conditions (15 kV, 1 nA), 295 K, focused beam (dotted line); 22 kV, 15 nA, 85 K, focused beam (dashed line); 22 kV, 15 nA, 85 K, defocused electron beam (solid line).

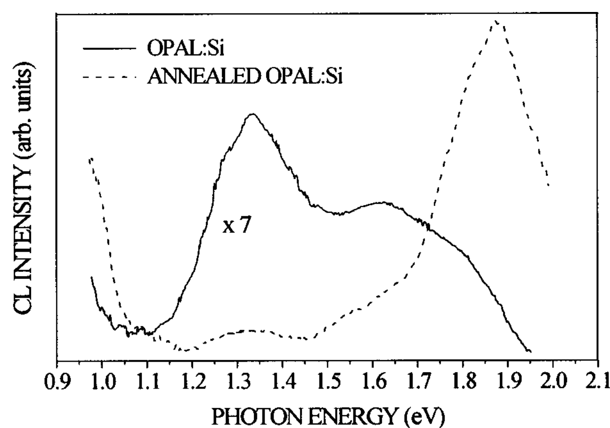

FIG. 4. Room temperature infrared CL spectra of opal:Si (solid line) and annealed opal:Si (dashed line) excited by an electron beam of 15 kV accelerating voltage and 1 nA current.

resolved bands peaked near 1.95 and 3.3–3.4 eV and the band centered at 2.7 eV appears as a shoulder of the dominant 3.3 eV emission (Fig. 2). In this case, Gaussian deconvolution indicates a shift towards higher energies of the previously observed bands, that now appear centered at 2.02, 2.40, 2.71, and 3.39 eV. Contrary to the nonannealed opals case, it was observed that the ratio $I_{CL}(1.9\,\mathrm{eV})/I_{CL}(3.4\,\mathrm{eV})$ decreased by increasing irradiation time.

B. Opal:Si

Visible CL is rather weak in opals infilled with Si and only after annealing at 800 °C it becomes clearly appreciated. Spectra recorded at room temperature with an accelerating voltage of 15 kV and beam currents of about 1 nA show an intense CL band centered at 1.95 eV as well as weaker luminescence in the (2.2–2.9) eV range (Fig. 3, dotted curve). This latter emission increases by increasing irradiation time, and appears centered at about 2.7 eV once saturation conditions have been reached. Spectra acquired under higher excitation conditions (20–25 kV, ~ 15 nA) or at low temperature (85 K) show emission bands at about 2.63–2.70 eV, 1.90 and 2.1–2.3 eV (Fig. 3, dashed curve). The 2.7 eV band dominates the spectrum and only when the SEM electron beam is defocused, i.e., the excitation density is reduced, the intensity of the 1.9 eV band exceeds the intensity of the 2.7 eV emission (Fig. 3, solid curve). A detailed Gaussian deconvolution of the spectra obtained at low temperature and/or under high excitation density reveals the existence of two additional bands centered near 2.90 and 3.25 eV, as well as the complex character of the 1.9 eV emission, which is really made up of two bands peaked at 1.91–1.93 and 1.81–1.86 eV. Main differences with spectra recorded under low excitation conditions or at room temperature are the dominant character of the 2.7 eV band and the appearance of a strong CL emission in the 2.9–3.3 eV range. We have actually found in CL spectra acquired at increasing temperatures that the intensity of the 2.7 eV band is reduced faster than the intensity of the 1.9 eV CL band. In addition, it was observed that an accelerating voltage decrease induces not only a CL intensity decrease, as expected, but also an increase of the $I_{CL}(1.9\,\mathrm{eV})/I_{CL}(2.7\,\mathrm{eV})$ ratio. The appearance of CL near 3.3 eV is probably connected with the use of a higher electron beam current, as supported by the CL observations carried out in annealed opals. The 2.9 eV band has been previously observed in crystalline SiO_2[5] and attributed to an irradiation produced intrinsic defect.

Si-infilled opals show, in addition, weak CL in the near infrared range at room temperature. As in the visible range, I_{CL} increases by increasing irradiation time. Corresponding spectra show a broad band peaked at about 1.34 eV and a weaker emission centered near 1.6 eV (Fig. 4). Upon annealing the spectrum becomes dominated by an intense 1.9 eV visible CL band, but emissions at 1.34 and 1.60 eV are still observed, as also shown in Fig. 4.

C. Opal:Pt

CL spectra of Pt-infilled opals are always dominated by a broad, complex band centered at about 2.3–2.55 eV. The CL maximum shifts towards higher energies by increasing exposure time to the SEM electron beam. In addition, an increase of the irradiation time induces the appearance of a resolved band at 1.95 eV and an enhancement of the CL

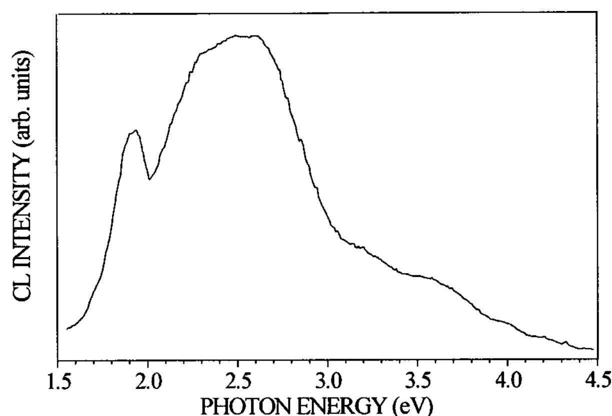

FIG. 5. CL spectra of an opal:Pt sample (15 kV, 1 nA, 295 K).

Downloaded 11 Oct 2013 to 147.96.14.16. This article is copyrighted as indicated in the abstract. Reuse of AIP content is subject to the terms at: http://jap.aip.org/about/rights_and_permissions

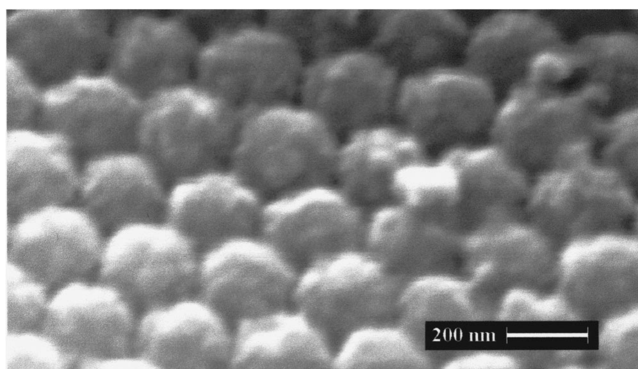

FIG. 6. High-resolution SEM image of an opal–Pt–Si composite.

emission in the (3.0–3.7) eV spectral range, where a shoulder of the main dominant emission can be appreciated near 3.4 eV (Fig. 5).

D. Opal–Pt–Si

Figure 6 shows a high-resolution SEM image of an opal–Pt–Si sample. A significant reduction of the opal pore volume was observed in these composites due to Si and Pt addition. Three samples infilled with Si and different amounts of Pt have been investigated. They were respectively labeled as opal–Pt–Si Nos. 1, 2, and 3 with increasing Pt content. Corresponding CL spectra are shown in Fig. 7. An intense, broad and complex band, centered at about 2.7 eV, always dominates the CL emission of the opal–Pt–Si composites irrespective of temperature, the accelerating voltage, or the beam current used to acquire the spectra. Emission bands at about, 1.88–1.90, 2.1–2.3, and 3.2 eV can also be appreciated, the first appears always resolved and the other two as shoulders of the main 2.7 eV band. Pt addition induces a considerable reduction of the CL intensity of the samples as compared with CL intensity of the opal:Si composites. A small Pt addition causes a strong reduction of the 1.9 eV band, while the intensity of the main 2.7 eV emission is reduced in a more gradual way by increasing the Pt content. In the sample with a higher Pt content (opal–Pt–Si No. 3) an enhancement of the 2.2 eV band is also clearly appreciated.

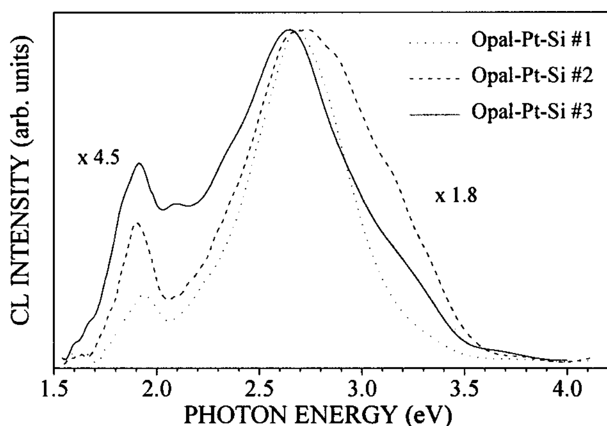

FIG. 7. CL spectra of the three opal–Pt–Si samples normalized to the intensity of the 2.7 eV band (25 kV, 15 nA, 85 K).

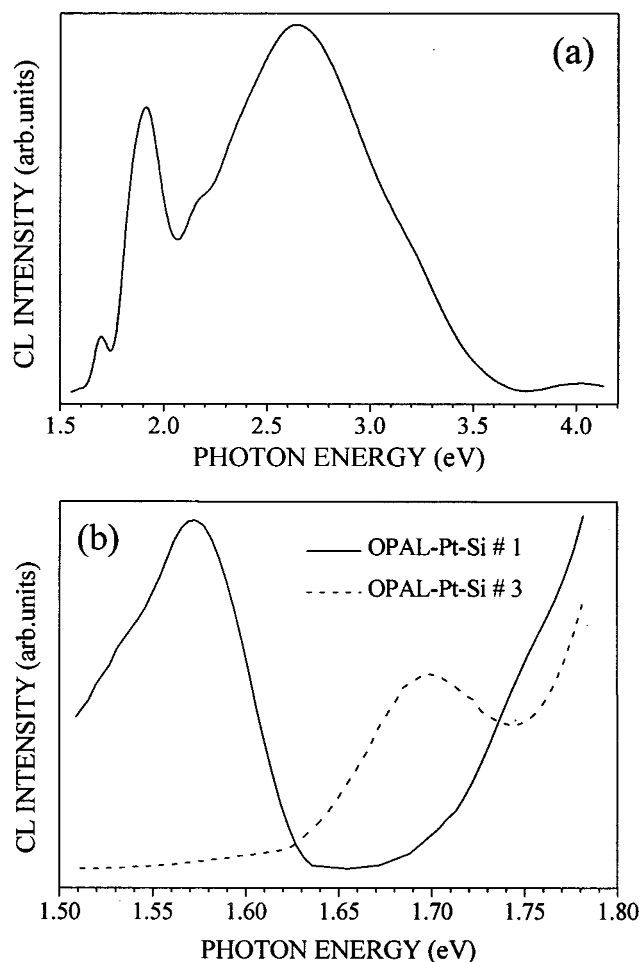

FIG. 8. (a) CL spectrum of opal–Pt–Si sample No. 3 showing a band at 1.70 eV related to Si nanocrystals. (b) Comparison of CL spectra of opal–Pt–Si sample Nos. 1 and 3 in the 1.5–1.8 eV spectral range (25 kV, 15 nA, 85 K). The CL intensity raise observed at higher energies is due to the presence of the 1.95 eV emission band.

Close to the low-energy limit of the visible spectral range, a weak CL band is frequently observed in several regions of the three opal–Pt–Si samples. The band is centered between 1.57 and 1.59 eV in samples opal–Pt–Si Nos. 1 and 2, and was observed peaked at the same energies in the opal:Si samples as well. However, in sample opal–Pt–Si No. 3 (highest Pt content) a similar band is found centered at about 1.70 eV. (Fig. 8).

Si and Pt distributions in the opal pores of opal–Pt–Si composites have been evaluated from electron probe microanalysis results. Near the surface the fill factor of Si is about 70% in volume and the fill factor of Pt is close to 25% in volume. While this latter is roughly constant across the composite the in-depth profile of the fill factor of Si is well-shaped (Fig. 9). Minimum fill factor values of Si were measured at about 100–150 μm depth depending on the surface considered. CL investigations carried out in cross sections of the same samples reveal a progressive enhancement of the CL intensity from the surfaces towards the interior. In fact,

Downloaded 11 Oct 2013 to 147.96.14.16. This article is copyrighted as indicated in the abstract. Reuse of AIP content is subject to the terms at: http://jap.aip.org/about/rights_and_permissions

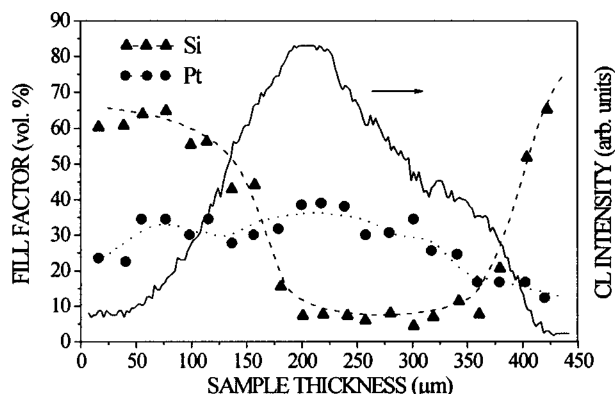

FIG. 9. CL intensity line profile (solid line) and dependence of fill factor of pores by Si (dashed line is a guide to the eye) and Pt (dotted line is a guide to the eye as well) measured along a cross section of an opal–Pt–Si sample.

CL intensity profiles measured in cross-sections of the opal–Pt–Si composites show the opposite trend than that shown by the Si fill factor profiles (Fig. 9). This comparison indicates that CL is enhanced as the concentration of Si embedded in the opal matrix decreases in depth. Such inhomogeneous CL intensity spatial distribution is clearly appreciated in the CL micrograph of an opal–Pt–Si sample cross section shown in Fig. 10 together with CL spectra acquired at different depths from the surface.

IV. DISCUSSION

The obtained results show that CL from the opal-based composites investigated in this work is strongly influenced by the material used to infill the opal pores and its concentration. The main features of the different bands observed in the samples will be discussed and compared in the following.

A. 3.4 eV band

A CL band centered at about 3.4 eV is observed in almost all the samples, although under different excitation conditions. A PL band at the same energy was observed by Liao *et al.*[19] in SiO_2 thin films and attributed to an unknown intrinsic defect. This band was also reported by Qin *et al.*[20] in oxidized porous silicon films and in SiO_2 powders annealed in oxygen at 1000 °C and attributed to some oxygen excess defect. PL at 3.4 eV has been also observed in amorphous Si:H:O films and assigned to oxygen related color centers in Si–O species.[21] Song *et al.*[22] proposed a two-fold coordinated Si defect (O–Si–O) at the interface between Si nanocrystals and a SiO_2 matrix as the luminescent center responsible for the 3.4 eV PL band observed in SiO_2 films. This PL was observed in as-deposited samples and strongly increased upon annealing the films at or above 800 °C.

The existence of nanosized silicon crystallites in opal silica spheres has been recently reported by Ajgaonkar *et al.*[23] This observation suggests that the presence of Si nanocrystals in our samples could be related to the 3.4 eV

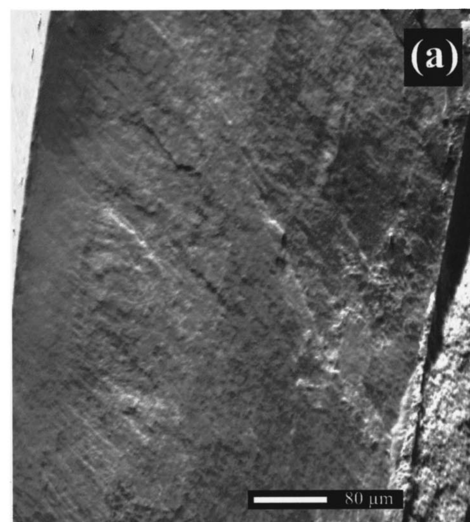

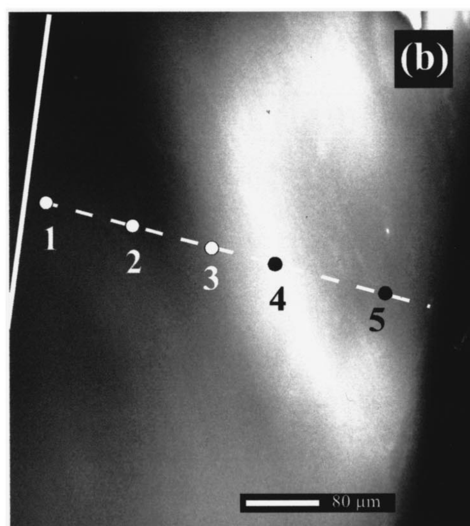

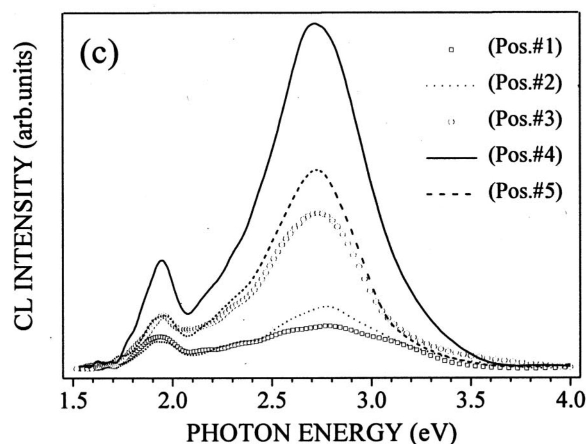

FIG. 10. (a) Secondary electron SEM image of an opal–Pt–Si composite cross section. (b) Corresponding CL image acquired at 85 K. The white line marks one of the edges of the sample. (c) CL spectra recorded at positions labeled 1–5 in (b) (22 kV, 15 nA, 85 K).

Downloaded 11 Oct 2013 to 147.96.14.16. This article is copyrighted as indicated in the abstract. Reuse of AIP content is subject to the terms at: http://jap.aip.org/about/rights_and_permissions

band with a mechanism similar to that proposed in Ref. 22 for the case of SiO_2 films. As in Ref. 22, we have found that the 3.4 eV band increases after annealing the samples at 800 °C (Fig. 2). In our samples the 3.4 eV band would be related to states at the interface between nanocrystals and the silica spheres of the opal.

B. 2.7 eV band

The 2.7 eV band is observed in all the opal-based composites, frequently as the dominant emission (Figs. 7, 8, and 10). This band has been extensively investigated and is usually attributed in amorphous SiO_2 to oxygen deficient centers, in particular to two-fold coordinated Si defects or to asymmetrically relaxed or unrelaxed neutral oxygen vacancies.[24,25] The two-fold coordinated Si defect is more disordered than the oxygen vacancy defect.[26] Due to the porous, disordered nature of the silica forming the opal spheres (as visualized in TEM images) and the structural disorder caused by irradiation, this defect seems in our case to occur with a higher probability than the oxygen vacancies. The coexistence of both kind of defects may explain the compound nature of the 2.7 eV band that can be clearly appreciated in several of the obtained spectra (Figs. 4 and 8). Enhancement of the 2.7 eV CL emission with increasing irradiation time or decreasing temperature agrees with previous CL studies of high-purity quartz[25] and thermally grown SiO_2 layers.[27]

C. Emission in the 2.15–2.45 eV range

CL in the 2.15–2.45 eV range observed in a-SiO_2 is usually attributed to radiative recombination of self-trapped excitons (STE),[5,6] i.e., correlated electron-hole pairs localized by self-induced lattice distortions. STE CL is very sensitive to local disorder. Experimental and theoretical investigations of STE in SiO_2 have led to a number of different models involving oxygen vacancies, peroxy linkages and E' centers (unpaired electron in a dangling tetrahedral sp^3 orbital of a single Si atom bonded to three oxygen atoms). STE are considered to be an interstitial-vacancy pair, for which the interstitial takes the form of an O_2 molecule.[28] PL at 2.25 eV observed[29] in irradiated bulk a-SiO_2 has been attributed to E'_{δ} centers, paramagnetic defects where an electron is delocalized over a cluster of five Si atoms. The generation process of oxygen vacancies and interstitials results in a structure quite similar to the five Si atoms cluster.[30] CL observed in our work in the 2.15–2.45 eV range can be tentatively related to the formation of Si nanoclusters, although it has not still been established if carrier recombination takes place inside these clusters or on the oxygen vacancy-oxygen interstitial pairs.[30] The formation of Si clusters in SiO_2 has been experimentally observed by means of Auger electron spectroscopy.[31,32] In the opal samples here investigated CL in the 2.15–2.45 eV range is enhanced by increasing irradiation time or excitation density, which supports the proposed relation between Si nanoclusters and the observed emission. This assignment also agrees with previous CL observations of SiO_2 films.[18] It is noteworthy to mention that enhanced 2.15–2.45 CL is observed in the opal:Pt samples and in opal–Pt–Si composites with a high Pt content (Figs. 6 and 8), which suggests that the $I_{CL}(2.2\,\mathrm{eV})/I_{CL}(2.7\,\mathrm{eV})$ ratio is favored by a reduced contact area between Si and SiO_2.

D. 1.9 eV band

The 1.9 eV band is usually related to nonbridging oxygen hole centers (NBOHC) defects.[5,25,33] The NBOHC is described as a hole trapped in a pure $2p\pi$ orbital of a single oxygen bonded to a single Si bonded to three oxygen atoms. Peroxy and hydroxyl linkages as well as strained silicon-oxygen bonds are possible precursors of these defects.[5,25,26] This variety of precursors explains the existence of two different NBOHC-related bands observed by deconvolution at about 1.91–1.93 and 1.81–1.86 eV. A clear enhancement of the 1.9 eV CL band intensity relative to the 2.7 eV emission intensity is observed in opal:Si samples by defocusing the electron beam (Fig. 3). This result agrees with previous CL observations in quartz[5] and confirms that 1.9 eV CL intensity changes are correlated with the power density in the interaction volume and, hence, with the electron beam-induced electric field.

E. Emission in the 1.50–1.75 eV range

CL appreciated in the 1.50–1.75 eV range (Fig. 9) can be attributed to Si nanocrystals, according to previous PL investigations, e.g., Refs. 34–36 and CL works.[10,37–39] CL emission appears centered between 1.57 and 1.61 eV in opal:Si and opal–Pt–Si sample Nos 1 and 2, while in sample opal–Pt–Si No. 3 (highest Pt content) it is peaked at 1.70 eV (Fig. 8). TEM measurements revealed the existence of Si nanocrystals of about 2 nm in size in the opal:Si and opal–Pt–Si samples, while nanocrystals with average size ranging 5–8 nm were observed in the annealed opal:Si composites[15,16] and also detected by Raman measurements.[16] Thus, although luminescence is related to Si nanocrystals, it cannot be attributed to a pure quantum confinement effect because no shift in the CL peak with the nanocrystal size is observed. According to TEM observations, Pt particles of several nm in size and in different stages of coalescence are distributed on the silica spheres surfaces.[15] Increasing Pt content then reduces the contact surface between Si and SiO_2. Our measurements show that a shift of the CL peak to higher energies is appreciated only when certain Pt concentration is reached. These observations support the possibility that the 1.5–1.7 eV CL is related to the existence of defect states at the interface between Si nanocrystals and SiO_2[35] and suggests that a high Pt addition modifies the electronic state of the mentioned defects. According to the model proposed in Ref. 35, the carrier generation occurs across the nanocrystal band gap while recombination takes place trough the lower-energy localized surface states. The energy of the photons emitted in this step depends on the surface state structure rather than on the nanocrystal size. On the other hand, Shimizu–Iwayama *et al.*[36,40] have also proposed that the interface energy state between Si nanocrystals and SiO_2 plays an essential role in the luminescence process and consider that this energy is affected by the nanocrystals interaction. Hence, the concentration of nanocrystals influences the lumi-

Downloaded 11 Oct 2013 to 147.96.14.16. This article is copyrighted as indicated in the abstract. Reuse of AIP content is subject to the terms at: http://jap.aip.org/about/rights_and_permissions

nescence emission. Our observation that the CL peak shifts to higher energies in the opal–Pt–Si sample No. 3 (Fig. 9), where a high density of Pt particles tends to separate the Si nanocrystals, can be explained by the model of Refs. 36 and 40. The slight increase of the 1.6 eV luminescence intensity observed in opal:Si samples after annealing agrees with an increased crystalline fraction of the embedded silicon, as supported by Raman measurements.[16]

F. Infrared CL

Infrared CL is observed in opal:Si samples at about 1.34 eV (Fig. 4). This luminescence is related to the existence of amorphous Si according to previous PL investigations.[8,41] Such assignment is supported by the reduction of the intensity of that CL band upon annealing the samples at 800 °C, and agrees with previous TEM observations.[15,16] In fact, about 90% of the Si embedded in the opal matrix is amorphous, while in annealed samples a mixture of amorphous and crystalline Si—with Si crystals of up to 300 nm in size—is shown by the mentioned TEM images.

V. CONCLUSIONS

The CL emission of synthetic opals infilled with Si (opal:Si), Pt (opal:Pt), as well as Si and different Pt contents (opal–Pt–Si samples) has been investigated. CL from the opal-based composites characterized in this work is strongly influenced by materials used to infill the opal pores and their concentration. X-ray microanalysis show an inhomogeneous distribution of Si in the opal matrix pores that induces changes in the luminescence intensity spatial distribution, as revealed by CL microscopy and spectroscopy.

The CL measurements indicate the existence of Si nanocrystals in the opal:Si and opal–Pt–Si composites. CL related to Si nanocrystals is observed in the 1.50–1.75 eV spectral range as a well-resolved band whose peak position depends on the Pt content of the samples. In fact, CL emission in the mentioned range is observed centered between 1.57 and 1.61 eV except in the opal–Pt–Si composite with the highest Pt content, where it is peaked at 1.70 eV. The behavior of this band together with previous TEM observations suggest that the CL emission is related to defect states at the interface between Si nanocrystals and SiO_2. The electronic state of these defects could be influenced by the interaction between nanocrystals. Another CL band centered near 3.4 eV is observed in bare opals and annealed opals as the dominant emission. This band seems to be included in the intense 2.7 eV emission in CL spectra of almost all the infilled opals. Our observations agree with previous assignment[22] of this band to two-fold coordinated Si defects also located at the interface between Si nanocrystals and the silica spheres of the opals. Infrared CL characteristic of amorphous silica has been detected in opal:Si samples.

ACKNOWLEDGMENTS

This work was supported by DGES (Project No. PB96-0639), the Russian R&D program ''Nanostructures'' (Grant No. 97-2016), and RFBR under Grant No. 98-02-17350.

[1] Yu. A. Vlasov, V. N. Astratov, O. Z. Karimov, and A. A. Kaplyanskii, Phys. Rev. B **55**, R13357 (1997).
[2] A. Blanco, C. López, R. Mayoral, H. Míguez, F. Meseguer, A. Mifsud, and J. Herrero, Appl. Phys. Lett. **73**, 1781 (1998).
[3] S. G. Romanov, A. V. Fokin, and R. M. De La Rue, Appl. Phys. Lett. **74**, 1821 (1999).
[4] D. L. Griscom, Phys. Rev. B **40**, 4224 (1989).
[5] M. A. Stevens Kalceff and M. R. Phillips, Phys. Rev. B **52**, 3122 (1995).
[6] C. Itoh, T. Suzuki, and N. Itoh, Phys. Rev. B **41**, 3794 (1990).
[7] L. Skuja, J. Non-Cryst. Solids **239**, 16 (1998).
[8] Y. Kanemitsu, M. Iiboshi, and T. Kushida, Appl. Phys. Lett. **76**, 2200 (2000).
[9] J. Piqueras, B. Méndez, R. Plugaru, G. Craciun, J. A. García, and A. Remón, Appl. Phys. A: Mater. Sci. Process. **68**, 329 (1999).
[10] T. Inokuma, Y. Kurata, and S. Hasegawa, J. Lumin. **80**, 247 (1999).
[11] W. Stöber, A. Fink, and E. Bohn, J. Colloid Interface Sci. **26**, 62 (1968).
[12] V. N. Bogomolov, L. S. Parfenieva, A. V. Prokofiev, I. A. Smirnov, S. M. Samoilovich, A. Jezowskii, J. Mucha, and H. Miserek, Phys. Solid State **37**, 1874 (1995).
[13] V. N. Bogomolov, L. M. Sorokin, D. A. Kurdyukov, T. M. Pavlova, and J. L. Hutchison, Phys. Solid State **39**, 1869 (1997).
[14] V. N. Bogomolov *et al.*, Tech. Phys. Lett. **24**, 326 (1998).
[15] N. A. Feoktistov, V. G. Golubev, J. L. Hutchison, D. A. Kurdyukov, A. B. Pevtsov, R. Schwarz, J. Sloan, and L. M. Sorokin, Mat. Res. Soc. Symp. Proc. **609**, A24.4.1 (2000).
[16] V. N. Bogomolov *et al.*, J. Non-Cryst. Solids **266–269**, 1021 (2000).
[17] C. Díaz-Guerra and J. Piqueras, Physica C **275**, 37 (1997).
[18] M. V. Zamoryanskaya and V. I. Sokolov, Phys. Solid State **40**, 1797 (1998).
[19] L.-S. Liao, X.-M. Bao, X.-Q. Zheng, N.-S. Li, and N.-B. Min, Appl. Phys. Lett. **68**, 850 (1996).
[20] G. G. Qin, J. Lin, J. Q. Duan, and G. Q. Yao, Appl. Phys. Lett. **69**, 1689 (1996).
[21] S. Tong, X.-N. Liu, T. Gao, and X.-M. Bao, Appl. Phys. Lett. **71**, 698 (1997).
[22] H. Z. Song, X. M. Bao, N. S. Li, and X. L. Wu, Appl. Phys. Lett. **72**, 356 (1998).
[23] M. Ajgaonkar, Y. Zhang, H. Grebel, M. Sosnowski, and D. C. Jacobson, Appl. Phys. Lett. **76**, 3876 (2000).
[24] H. Imai, K. Araki, and H. Imagawa, Phys. Rev. B **38**, 12772 (1988).
[25] M. A. Stevens Kalceff, Phys. Rev. B **57**, 5674 (1998).
[26] D. L. Griscom, J. Appl. Phys. **77**, 5008 (1995).
[27] X. Liu, J. C. H. Phang, D. S. H. Chan, and W. K. Chim, J. Phys. D **32**, 1563 (1999).
[28] R. Tohmon, Y. Shimogaichi, H. Mizuno, Y. Ohki, K. Nagasawa, and Y. Hama, Phys. Rev. Lett. **62**, 1388 (1989).
[29] W. Hayes, M. J. Kane, O. Salminen, R. L. Wood, and S. P. Doherty, J. Phys. C **17**, 2943 (1984).
[30] M. Watanabe, S. Juodkazis, H. B. Sun, S. Matsuo, and H. Misawa, Phys. Rev. B **60**, 9959 (1999).
[31] S. Thomas, J. Appl. Phys. **45**, 161 (1974).
[32] B. Carrière and B. Lang, Surf. Sci. **64**, 209 (1977).
[33] L. N. Skuja, A. R. Silin, and A. G. Boganov, J. Non-Cryst. Solids **63**, 431 (1984).
[34] A. G. Cullis, L. T. Canham, and P. D. J. Calcott, J. Appl. Phys. **82**, 909 (1997).
[35] Y. Kanemitsu, Phys. Rev. B **49**, 16845 (1994).
[36] T. Shimizu-Iwayama, D. E. Hole, and I. W. Boyd, J. Phys.: Condens. Matter **11**, 6595 (1999).
[37] A. G. Cullis, L. T. Canham, G. M. Williams, P. W. Smith, and O. D. Doser, J. Appl. Phys. **75**, 493 (1994).
[38] J. Rams, B. Méndez, G. Craciun, R. Plugaru, and J. Piqueras, Appl. Phys. Lett. **74**, 1728 (1999).
[39] J. Rams, R. Plugaru, and J. Piqueras, Mater. Sci. Eng., B **68**, 126 (1999).
[40] T. Shimizu-Iwayama, N. Kurumado, D. E. Hole, and P. D. Townsend, J. Appl. Phys. **83**, 6018 (1998).
[41] D. Han, G. Yue, J. D. Lorentzen, and J. Lin, J. Appl. Phys. **87**, 1882 (2000).

Downloaded 11 Oct 2013 to 147.96.14.16. This article is copyrighted as indicated in the abstract. Reuse of AIP content is subject to the terms at: http://jap.aip.org/about/rights_and_permissions